scientific reports

Check for updates

OPEN

Periodic arrangements of tetrahedra having appearances similar to that of the Boerdijk–Coxeter helix

Susumu Onaka

The Boerdijk–Coxeter helix (BC helix or tetrahelix) is a linear stacking of regular tetrahedra. Although the BC helix exhibits an aperiodic nature, structures resembling the BC helix with periodicity are found in materials. To understand such structures, we considered a modification of the BC helix to introduce periodicity. By adjusting the relative rotation of adjacent tetrahedra, we demonstrated that periodic arrangements consisting of 8, 11, and 14 tetrahedra have appearances similar to that of the BC helix.

Keywords Boerdijk–Coexester helix, Tetrahelix, Regular tetrahedron, Twinning, Nanowire, Structure model

A well-known linear stacking of regular tetrahedra is the Boerdijk–Coxeter helix (BC helix or tetrahelix), where equilateral triangle faces coincide between adjacent tetrahedra[1–7]. The BC helix has two chiral forms depending on the direction of winding[4–6], and the one illustrated in Fig. 1 is left-handed.

Interestingly, structures resembling the BC helix are found in materials[4,5,7–13]. For example, the structures of some helical biomolecules are described as derivatives of the BC helix[4]. The structure resembling the BC helix has also been identified in the structure of crystals of simple inorganic materials. Previous studies determined that the structure of the close-packed metallic β-Mn crystal is a primitive cubic lattice of such helix[7–9]. Additionally, high-resolution electron microscopy revealed that the BC helix is a suitable structural model for thin metal nanowires[5,10,11].

The BC helix is known to exhibit an aperiodic nature, lacking rotational symmetry[1–6]. However, in crystalline solids, constituents are arranged periodically, and structures resembling the BC helix with periodicity have been reported[5,7–9,12]. To understand such structures, modifications of the BC helix to introduce periodicity have been considered. Sadler et al.[6] explored these modified BC helices, where tetrahedra rejoin in the same orientation. They designated the modified BC helix with periodicity as the *N*-BC helix (*N* being the number of tetrahedra in the unit of periodicity)[6]. However, Sadler et al. only illustrated two modified BC helices: the 3- and 5-BC helices[6]. As noted by Read[14], the appearances of the 3- and 5-BC helices are jagged and quite different from that of the original BC helix. In this study, we consider the appearances of the modified helix and show that 8-, 11- and 14-BC helices have appearances similar to that of the BC helix. The present results provide basic knowledge to discuss structures resembling the BC helix in materials.

Crystallographic method of analysis to construct the BC helix

We construct the BC helix from a crystallographic perspective for materials with an FCC structure. Figure 2 illustrates two grains with identical orientations depicted by two tetrahedra. To depict the tetrahedra, equations giving shapes of convex polyhedra derived by Onaka[15] are used. The two tetrahedra in Fig. 2 possess {111} parallel planes with normal vectors pointing in opposite directions, such as [111] and $[\bar{1}\bar{1}\bar{1}]$ or $[1\bar{1}\bar{1}]$ and $[\bar{1}11]$. By rotating the right tetrahedron by $\pi/3$ about the [111] axis, it represents a twinned Σ3 orientation relative to the left parent orientation. This becomes a fundamental unit in the BC helix.

Repeated twinning under certain conditions forms the BC helix, and Fig. 3 shows the procedure for that with a left-handed arrangement. The green tetrahedra represent the parent grains (PGs). As the first step of repeated twinning, the red tetrahedra in Fig. 3 represent the first-order twin (T1), caused by a $\pi/3$ rotation about the [111] axis of the parent grains. For this case, (111) of PG is a coherent twin boundary (CTB) between PG and T1. As well as the first-order twinning where we chose (111) as CTB, there are three possible CTB between T1 and the blue tetrahedra (T2). In Fig. 3, $(1\bar{1}\bar{1})_{T1}$ is selected as CTB and T2 is caused by a $\pi/3$ rotation about the

Department of Materials Science and Engineering, Tokyo Institute of Technology, 4259-J2-63 Nagatsuta, Yokohama 226-8502, Japan. email: onaka.s.aa@m.titech.ac.jp

Figure 1. The Boerdijk-Coexester helix (BC helix) with a left-handed arrangement. Equilateral triangle faces coincide between adjacent tetrahedra. We made 3D images in this figure by using "Wolfram Mathematica, ver. 13.1.0.0 (https://www.wolfram.com/mathematica/).

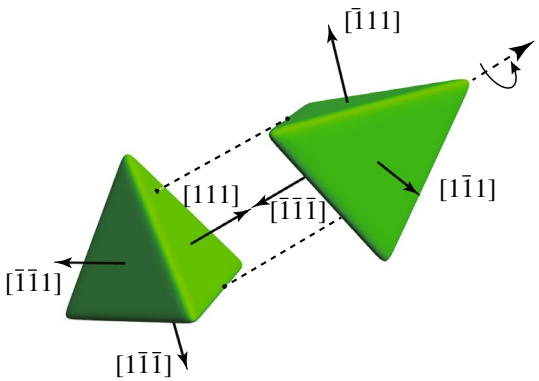

Figure 2. Two tetrahedra surrounded by {111} planes showing two grains with identical orientations. We made 3D images in this figure by using "Wolfram Mathematica, ver. 13.1.0.0 (https://www.wolfram.com/mathematica/).

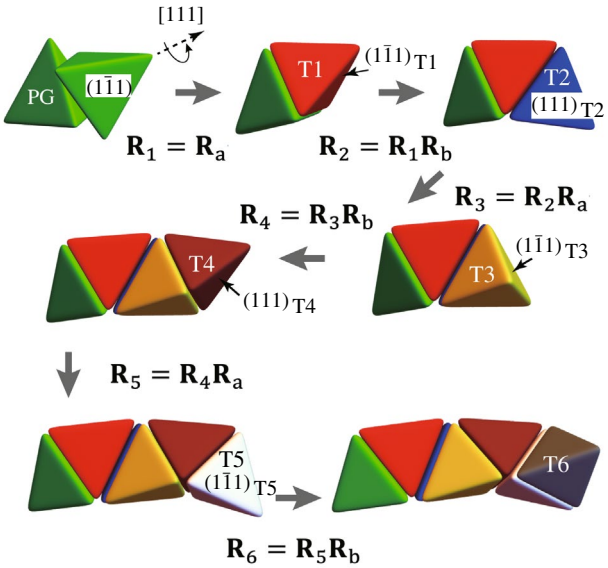

Figure 3. Repeated twinning to form the BC helix with a left-handed arrangement. The green tetrahedra represent the parent grains, and the red and blue tetrahedra represent the first-order (T1) and the second-order (T2) twins, respectively. Following higher-order twining is also shown. For the operations shown by $\mathbf{R}_m(m$: integer), see text. We made 3D images in this figure by using "Wolfram Mathematica, ver. 13.1.0.0 (https://www.wolfram.com/mathematica/).

$[1\bar{1}1]_{T1}$ axis of the red tetrahedron (T1). This is the second step of repeated twinning. Following the first and second steps, $(111)_{T2}$ of the blue tetrahedra (T2) is selected as CTB and T3 is caused by a $\pi/3$ rotation about the $[111]_{T2}$ axis of the blue tetrahedron (T2). In Fig. 3, repeated twinning with CTBs of alternating (111) and $(1\bar{1}1)$ are represented by tetrahedra with different colors up to the sixth-order twinning. This is the procedure to construct the BC helix with a left-handed arrangement from a crystallographic perspective.

Here we describe the sequence of twinning shown in Fig. 3 by using rotation matrices. The rotation matrix $\mathbf{N}$ for the rotation around the unit vector $\mathbf{v} = (v_1, v_2, v_3)$ by the angle θ is written as

$$\mathbf{N}(\mathbf{v},\theta)=\begin{pmatrix}\left(1-v_1^2\right)\cos\theta+v_1^2 & v_1v_2(1-\cos\theta)-v_3\sin\theta & v_3v_1(1-\cos\theta)+v_2\sin\theta\\ v_1v_2(1-\cos\theta)+v_3\sin\theta & \left(1-v_2^2\right)\cos\theta+v_2^2 & v_2v_3(1-\cos\theta)-v_1\sin\theta\\ v_3v_1(1-\cos\theta)-v_2\sin\theta & v_2v_3(1-\cos\theta)+v_1\sin\theta & \left(1-v_3^2\right)\cos\theta+v_3^2\end{pmatrix}. \quad (1)$$

We define the rotation matrix $\mathbf{R}_a$ so that it gives the orientation of T1 with respect to PG. Then, $\mathbf{R}_a$ is written as $\mathbf{N}(\mathbf{v},\theta)$ with $\mathbf{v}_a=(1,1,1)/\sqrt{3}$ and $\theta=\pi/3$. We also define the rotation matrix $\mathbf{R}_b$ so that it gives the orientation of T2 with respect to T1. Then, $\mathbf{R}_b$ is written as $\mathbf{N}(\mathbf{v},\theta)$ with $\mathbf{v}_b=(1,-1,1)/\sqrt{3}$ and $\theta=\pi/3$. Using Eq. (1), these are respectively written as

$$\mathbf{R}_a=\mathbf{N}(\mathbf{v}_a,\pi/3)=\frac{1}{3}\begin{pmatrix}2&-1&2\\2&2&-1\\-1&2&2\end{pmatrix} \quad (2)$$

and

$$\mathbf{R}_b=\mathbf{N}(\mathbf{v}_b,\pi/3)=\frac{1}{3}\begin{pmatrix}2&-2&-1\\1&2&-2\\2&1&2\end{pmatrix}. \quad (3)$$

The rotation matrix $\mathbf{R}_1$ to give the orientation of T1 with respect to PG is $\mathbf{R}_a$ itself and $\mathbf{R}_1=\mathbf{R}_a$, The rotation matrix $\mathbf{R}_2$ to give the orientation of T2 with respect to PG is $\mathbf{R}_2=\mathbf{R}_1\mathbf{R}_b=\mathbf{R}_a\mathbf{R}_b$. Then, the rotation matrix $\mathbf{R}_m$ (m: natural number) to give the orientation of Tm with respect to PG is written as

$$\begin{aligned}&\mathbf{R}_m=\mathbf{R}_a \text{ when } m=1,\\ &\mathbf{R}_m=\mathbf{R}_{m-1}\mathbf{R}_b \text{ when } m \text{ is even},\\ &\mathbf{R}_m=\mathbf{R}_{m-1}\mathbf{R}_a \text{ when } m(>1) \text{ is odd}.\end{aligned} \quad (4)$$

The rotation matrix $\mathbf{R}_m$ corresponds to the $\Sigma 3^m$ relations, which describes the orientation relationship in twin-related domain[16]. The concept of the $\Sigma 3^m$ relations has been used in the field of metallurgy[16]. For $\mathbf{R}_m$ to form the BC helix, the correspondence between $\mathbf{R}_m$ and $\Sigma 3^m$ for $m\le 6$ is written as shown below.

$$\mathbf{R}_1:\Sigma 3,\quad \mathbf{R}_2:\Sigma 9,\quad \mathbf{R}_3:\Sigma 27\text{b},\quad \mathbf{R}_4:\Sigma 81\text{b},\quad \mathbf{R}_5:\Sigma 243\text{g},\quad \mathbf{R}_6:\Sigma 729\text{m}. \quad (5)$$

Alphabet after the Σ value such as b of Σ27b shows subtypes of the Σ relations and the above notation of subtypes follows that shown in the paper by Cayron[16].

Using $\mathbf{R}_m$, normal directions of CTBs within the BC helix are calculated. Figure 4 is a 100 standard stereographic projection (SP) with respect to PG. The small circular symbols represent normal directions of CTBs within the BC helix, originating from [111] direction of PG. First ten directions are denoted by close symbols

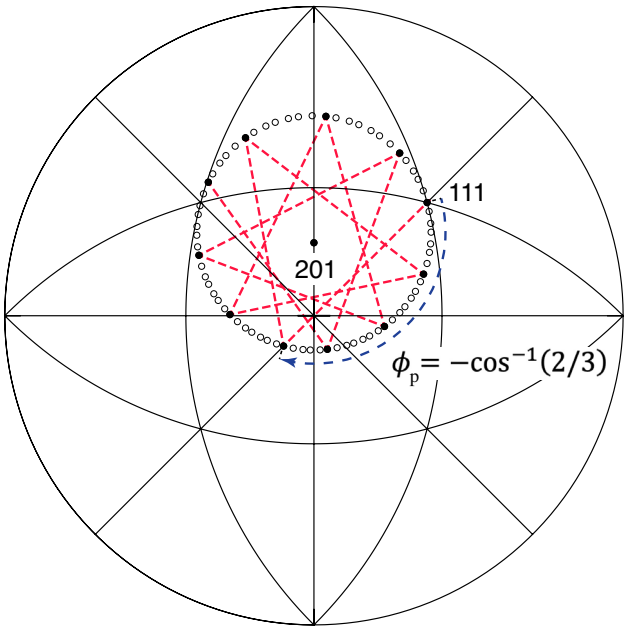

Figure 4. Stereographic projection showing the variation of normal directions of coherent twin boundaries (CTBs) within the BC helix with a left-handed arrangement. The small circular symbols represent the changes in the normal directions of CTBs, originating from [111] direction of the parent grain. First ten directions are denoted by close symbols connected by broken red lines, while the subsequent fifty-eight directions are represented by open symbols.

connected by broken red lines, while the subsequent fifty-eight directions are represented by open symbols. No parallel CTBs exist because of the aperiodicity of the BC helix.

Figure 4 also illustrates that the normal directions of CTBs rotate around [201] direction of the parent grain[3], with a rotation angle of $-\cos^{-1}[-2/3] \approx -131.81°$[4–6]. This angle is also a rotation angle of tetrahedra around [201] direction of the parent grain, and the [201] direction is an elongation direction of the BC helix[3]. The product $\mathbf{R}_p$ of the rotation matrices $\mathbf{R}_a$ and $\mathbf{R}_b$ given by Eqs. (2) and (3) is written as

$$\mathbf{R}_p = \mathbf{R}_a\mathbf{R}_b = \frac{1}{9}\begin{pmatrix} 7 & -4 & 4 \\ 4 & -1 & -8 \\ 4 & 8 & 1 \end{pmatrix}. \tag{6}$$

The product $\mathbf{R}_p$ is considered to be a combination of the unit operations to construct the BC helix. The [201] direction of the BC helix is understood to be the eigenvector $\mathbf{E}_p = (2, 0, 1)$ of $\mathbf{R}_p$. Actually, using the rotation angle $\phi_p = -\cos^{-1}(-2/3)$ around the eigenvector $\mathbf{E}_p$ of $\mathbf{R}_p$, $\mathbf{R}_p$ is rewritten from Eq. (1) as

$$\mathbf{R}_p = \mathbf{N}(\mathbf{e}_p, 2\phi_p) = \frac{1}{9}\begin{pmatrix} 7 & -4 & 4 \\ 4 & -1 & -8 \\ 4 & 8 & 1 \end{pmatrix} \tag{7}$$

where

$$\mathbf{e}_p(\pi/3) = (2, 0, 1)/\sqrt{5} \tag{8}$$

is the unit vector parallel to $\mathbf{E}_p = (2, 0, 1)$. The factor 2 in Eq. (7) in front of ϕ_p is needed since the rotation matrix $\mathbf{R}_p$ is that for two tetrahedra.

Modification of the BC helix

The rotation angle θ of tetrahedra around <111> to construct the BC helix is $\pi/3$. We can modify the BC helix by changing θ from $\pi/3$. Instead of $\mathbf{R}_a = \mathbf{N}(\mathbf{v}_a, \pi/3)$, $\mathbf{R}_b = \mathbf{N}(\mathbf{v}_b, \pi/3)$ and the product $\mathbf{R}_p = \mathbf{R}_a\mathbf{R}_b$, we consider

$$\begin{aligned} \mathbf{R}_A &= \mathbf{N}(\mathbf{v}_a, \theta) \text{ where } \mathbf{v}_a = (1, 1, 1)/\sqrt{3}, \\ \mathbf{R}_B &= \mathbf{N}(\mathbf{v}_a, \theta) \text{ where } \mathbf{v}_b = (1, -1, 1)/\sqrt{3}, \end{aligned} \tag{9}$$

and their product

$$\mathbf{R}_P(\theta) = \mathbf{R}_A\mathbf{R}_B.$$

The product $\mathbf{R}_P(\theta)$ is a function of θ and the eigenvector $\mathbf{E}_P$ of $\mathbf{R}_P(\theta)$ is written as

$$\mathbf{E}_P(\theta) = (d, 0, 1) = \left(\frac{2[1 + \sin(\theta + \pi/6)]}{1 + 2\cos\theta}, 0, 1\right). \tag{10}$$

The unit vector $\mathbf{e}_U(\theta)$ parallel to $\mathbf{E}_U(\theta)$ is written as

$$\mathbf{e}_P(\theta) = (\alpha, 0, \beta), \tag{11}$$

where

$$\alpha = \frac{\sqrt{1 + \cos(\theta - \pi/3)}}{\sqrt{2 + \cos\theta}} \text{ and } \beta = \frac{(1 + 2\cos\theta)}{2\sqrt{(2 + \cos\theta)[1 + \cos(\theta - \pi/3)]}}. \tag{12}$$

Figure 5 shows the changes of α and β as a function of θ. As shown by Fig. 5, we have

$$(\alpha, 0, \beta) \to (1, 0, 1)/\sqrt{2} \text{ when } \theta \to 0 \tag{13}$$

and

$$(\alpha, 0, \beta) \to (1, 0, 0) \text{ when } \theta \to 2\pi/3\,(= 120°). \tag{14}$$

The rotation angle ϕ_P of tetrahedra around the direction $\mathbf{E}_P(\theta)//\mathbf{e}_P(\theta)$ is also a function of θ. Using $\mathbf{e}_P(\theta)$ and ϕ_P, we have

$$\mathbf{R}_P(\theta) = \mathbf{N}(\mathbf{e}_P(\theta), 2\phi_P). \tag{15}$$

Using this relationship and Eq. (1), we can calculate ϕ_P as a function of θ as shown by Fig. 6.

Appearances of the modified BC helices

For certain values of θ and ϕ_P, the modified BC helix has the periodicity. Figure 7 is a 100 stereographic projection with respect to PG, showing normal directions of boundaries between tetrahedra in the modified BC helix, when

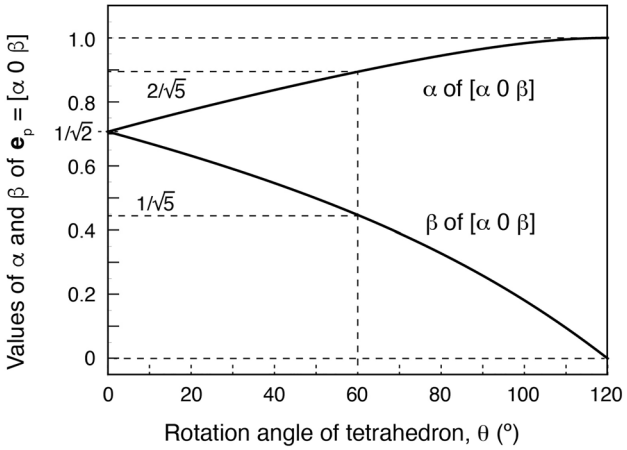

Figure 5. The variations of the components α and β of the eigenvector $\mathbf{e}_P(\theta) = (\alpha, 0, \beta)$ as a function of the rotation angle θ of tetrahedron around $< 111 >$.

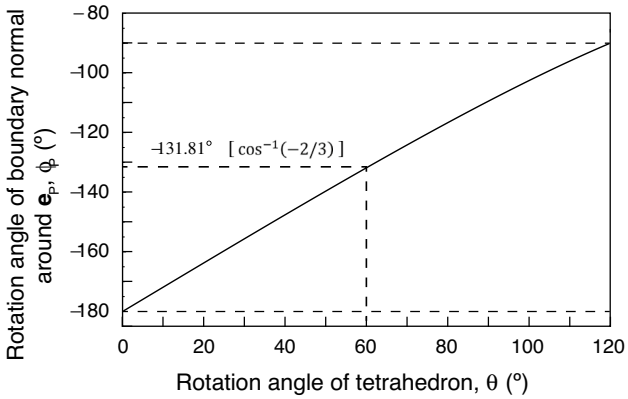

Figure 6. The relationship between the rotation angle θ of tetrahedron around 111 and the rotation angle ϕ_P of the tetrahedron around $\mathbf{E}_P(\theta) = (d, 0, 1)//\mathbf{e}_P(\theta) = (\alpha, 0, \beta)$.

$$\theta = \tan^{-1}\left[\frac{\sqrt{39+48\sqrt{2}}}{7}\right]\left(\approx 55.90^\circ\right) \text{ and } \phi_P = -3\pi/4 (= -135^\circ). \tag{16}$$

The value of d of $(d, 0, 1)$ for this case is

$$d = \left(1 + \sqrt{2} + \sqrt{2\sqrt{2}-1}\right)/2 \approx 1.88. \tag{17}$$

The periodicity of this modified BC helix is $N = 8$ and this is shown by the figure made by connecting the normal directions in Fig. 7. The angle $\phi_P = -3\pi/4$ causes the figure of a regular star polygon represented by {8/3} using the Schläfli symbol when $(d, 0, 1)$ is located at the center of SP. Figure 8a shows the appearance of this 8-BC helix. In Fig. 8a, eight colors are used to emphasize the periodicity $N = 8$. The 8-BC helix has an appearance very similar to that of the BC helix shown in Fig. 1.

When there is no restriction about N, there are many modified BC helices with periodicity. We hence focus on two other modified BC helices having both short periodicity and appearances similar to that of the original BC helix. One is the 11-BC helix and the other is the 14-BC helix. Their appearances are illustrated using 11 or 14 colors in Fig. 8b and c, respectively. Details of the 8-, 11- and 14-BC helices such as values of θ and ϕ_P are tabulated in Table 1.

As described in Introduction, 3-BC and 5-BC helices are the modified helices shown by Salder et al.[6]. The 3-BC and 5-BC helices have been reproduced by the present method of analysis, with their details and appearances respectively shown in Table 1 and Fig. 8. Unlike the 8-, 11- and 14-BC helices reported in the present study, the 3-BC and 5-BC helices have jagged appearances compared to the BC helix, as shown in Fig. 8d and e.

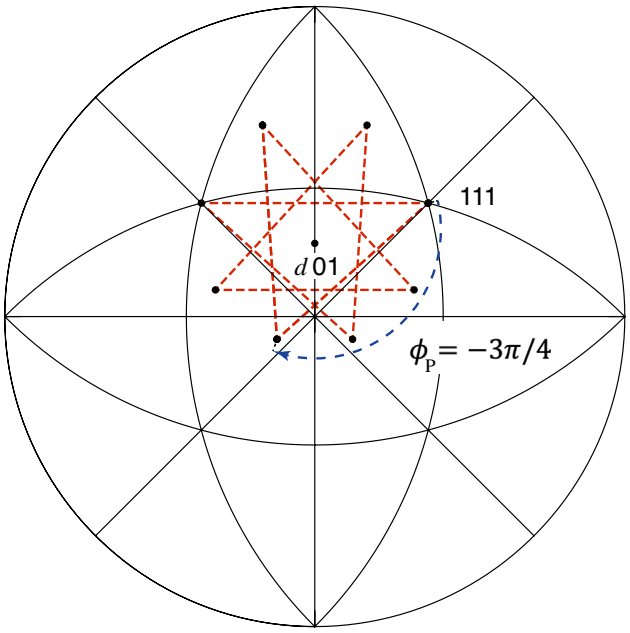

Figure 7. Stereographic projection showing the variation of normal directions of boundaries within the modified BC helix with the periodicity of $N = 8$. The figure connecting the normal directions of boundaries of tetrahedra becomes a regular star polygon represented by {8/3} using the Schläfli symbol when $(d, 0, 1)$ is located at the center of the stereographic projection.

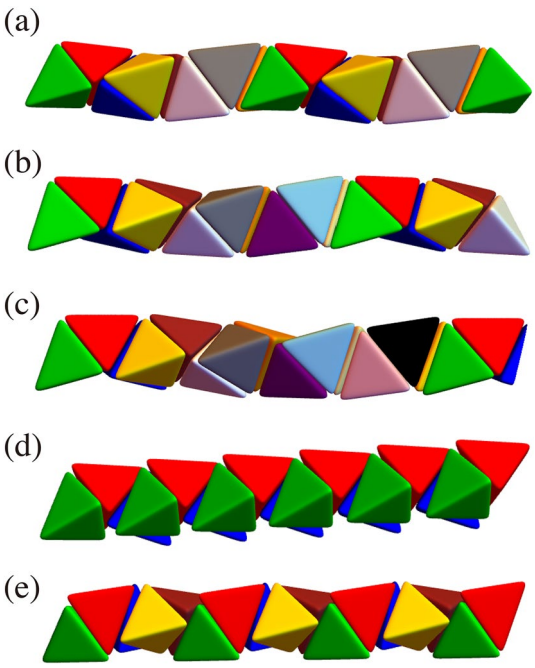

Figure 8. Appearances of (**a**) 8-BC, (**b**) 11-BC, (**c**) 14-BC, (**d**) 3-BC and (**e**) 5-BC helices. We made 3D images in this figure by using "Wolfram Mathematica, ver. 13.1.0.0 (https://www.wolfram.com/mathematica/).

Structures resembling the BC helix are found in materials[5,7–13] as mentioned in Introduction. In such structures, 8- and 11-unit of tetrahedra are frequently observed[5,7–9,12]. In the present paper, we modified the BC helix by considering the relative rotation of adjacent tetrahedra at boundaries and showed that periodic arrangements consisting of 8, 11, and 14 tetrahedra have appearances similar to that of the BC helix.

The present method of modification disrupts the edge-to-edge and vortex-to-vortex correspondence at boundaries of adjacent tetrahedral units within the helix. When a tetrahedral unit within the helix consists of

Name, Schläfli symbol	Rotation angle θ	Rotation angle φ	d of [d 0 1]
BC helix, None	$\pi/3 (= 60°)$	$-\cos^{-1}(-2/3)$ $(\approx -131.81°)$	2
8-BC helix, {8/3}	$\tan^{-1}\left[\frac{\sqrt{39+48\sqrt{2}}}{7}\right]$ $(\approx 55.90°)$	$-3\pi/4$ $(= -135°)$	$\left(1+\sqrt{2}+\sqrt{2\sqrt{2}-1}\right)/2$ ≈ 1.88
11-BC helix, {11/4}	$\tan^{-1}\left[\frac{\sqrt{3(4+4\beta-3\beta^2)}}{3\beta-2}\right]$ where $\beta=\sqrt{2-2\sin\left(\frac{\pi}{22}\right)}$ $(\approx 61.16°)$	$-8\pi/11$ $(\approx -130.91°)$	$\frac{2+\beta+\sqrt{4+4\beta-3\beta^2}}{2\beta}$ where $\beta=\sqrt{2-2\sin\left(\frac{\pi}{22}\right)}$, ≈ 2.04
14-BC helix, {14/5}	$\tan^{-1}\left[\frac{\sqrt{3(4+4\beta-3\beta^2)}}{3\beta-2}\right]$ where $\beta=\sqrt{2-2\sin\left(\frac{\pi}{14}\right)}$ $(\approx 64.20°)$	$-5\pi/7$ $(\approx -128.57°)$	$\frac{2+\beta+\sqrt{4+4\beta-3\beta^2}}{2\beta}$ where $\beta=\sqrt{2-2\sin\left(\frac{\pi}{14}\right)}$, ≈ 2.14
3-BC helix, {3}	$\tan^{-1}\left[\sqrt{15}\right]=\cos^{-1}[1/4]$ $(\approx 75.52°)$	$-2\pi/3$ $(= -120°)$	$(3+\sqrt{5})/2 \approx 2.62$
5-BC helix, {5/2}	$(2\pi/3)-\cos^{-1}[1/4]$ $(\approx 44.48°)$	$-4\pi/5$ $(= -144°)$	$(1+\sqrt{5})/2 \approx 1.62$

Table 1. Details of the BC helix, the 8-, 11- and 14-BC helices having both short periodicity and similar appearances to the BC helix, and the 3- and 5-BC helices. For each helix, the Schläfli symbol for the figure made by connecting boundary normals in stereographic projection, the rotation angle θ of tetrahedron around $<111>$, the rotation angle φ of tetrahedron around [d 0 1] and the d value of [d 0 1] are shown.

several hundred atoms, as observed in nanowires, relaxation mechanisms such as the generation of crystal defects or diffusion may occur near the boundaries. However, the crystal structure inside the tetrahedral units remains intact. On the other hand, in materials such as β-Mn and certain organic compounds, which exhibit structures similar to the BC helix with periodicity, tetrahedral units consist of vertex-bound atoms[7–9,12]. While experimental data on atomic arrangements in such helices are available[7–9,12], our study is theoretical in nature, employing a continuum approximation and geometrical analysis. Although specific crystallographic details such as atomic coordinates are not given by the present study, we believe our approach of modifying the BC helix by considering relative tetrahedral rotations is valuable for exploring structures resembling the BC helix with periodicity.

Conclusions

The Boerdijk–Coxeter helix (BC helix or tetrahelix) is a linear stacking of regular tetrahedra. Although the BC helix exhibits an aperiodic nature, structures resembling the BC helix with periodicity are found in real materials. We have modified the BC helix by considering the relative rotation of adjacent tetrahedra, and shown that periodic arrangements consisting of 8, 11, and 14 tetrahedra have appearances similar to that of the BC helix.

Data availability

The datasets used and/or analyzed during the current study available from the corresponding author on reasonable request.

Received: 28 May 2024; Accepted: 31 July 2024
Published online: 06 August 2024

References

1. Coxeter, H. S. M. *Regular Complex Polytopes* (Cambridge University, 1974).
2. Boerdijk, A. H. Some remarks concerning close-packing of equal spheres. *Philips Res. Rep.* **7**, 303–313 (1952).
3. Lord, E. A. & Ranganathan, S. Shape packing, helices and the polytope {3,3,5}. *Eur. Phys. J. D* **15**, 335–343 (2001).
4. Sadoc, J. F. & Rivier, N. Boerdijk–Coxeter helix and biological helices. *Eur. Phys. J. B* **12**, 309–318 (1999).
5. Zhu, Y. *et al.* Chiral gold nanowires with Boerdijk–Coxeter–Bernal structure. *J. Am. Chem. Soc.* **136**, 12746–12752 (2014).
6. Sadler, G. *et al.* Periodic modification of the Boerdijk–Coxeter helix (tetrahelix). *Mathematics* **7**, 1001 (2019).
7. Talis, A., Everstov, A. & Kraposhin, V. Crystal structures of alpha and beta modifications of Mn as packing of tetrahedral helices extracted from a four-dimensional 3,3,5 polytope. *Acta Cryst.* **B76**, 948–954 (2020).
8. Talis, A., Everstov, A. & Kraposhin, V. Spiral tetrahedral packing in the β-Mn crystal as symmetry realization of the 8D E8 lattice. *Acta Cryst.* **A77**, 7–18 (2021).
9. Talis, A. & Kucherinenko, Y. Non-crystallographic helices in polymers and close-packed metallic crystals determined by the four-dimensional concept of the icosahedron. *Acta Cryst.* **B79**, 537–546 (2023).
10. Pacheco-Contreras, R. *et al.* Tetrahelix conformations and transformation pathways in Pt_1Pd_{12} clusters. *J. Phys. Chem. A* **116**, 5235–5239 (2012).
11. Chang, F. *et al.* Strain-modulated platinum–palladium nanowires for oxygen reduction reaction. *Nano Lett.* **20**, 2416–2422 (2020).
12. Xiao, Q., Wu, Y., Li, M., O'Keeffe, M. & Li, D. A metal-organic framework with rod secondary building unit based on the Boerdijk–Coxeter helix. *Chem. Commun.* **52**, 11543–11546 (2016).
13. Schoedel, A., Li, M., Li, D., O'Keeffe, M. & Yaghi, O. M. Structure of metal-organic frameworks with rod secondary building units. *Chem. Rev.* **116**, 12466–12535 (2016).
14. Read, R. L. Calculating the segmented helix formed by repetitions of identical subunits thereby generating a zoo of platonic helices. *Mathematics* **10**, 2533 (2022).

15. Onaka, S. Simple equations giving shapes of various convex polyhedra: The regular polyhedra and polyhedra composed of crystallographically low-index planes. *Philos. Mag. Lett.* **86**, 175–183 (2006).
16. Cayron, C. Multiple twinning in cubic crystals: Geometric/algebraic study and its application for the identification of the Σ3n grain boundaries. *Acta Cryst.* **63**, 11–29 (2007).

Author contributions
This is my own work and there is no co-author.

Funding
This work was supported by JSPS KAKENHI Grant Number 22K04668.

Competing interests
The author declares no competing interests.

Additional information
Correspondence and requests for materials should be addressed to S.O.

Reprints and permissions information is available at www.nature.com/reprints.

Publisher's note Springer Nature remains neutral with regard to jurisdictional claims in published maps and institutional affiliations.